JACS
JOURNAL OF THE AMERICAN CHEMICAL SOCIETY
Article
pubs.acs.org/JACS

Initial Light Soaking Treatment Enables Hole Transport Material to Outperform Spiro-OMeTAD in Solid-State Dye-Sensitized Solar Cells

Lei Yang,[†,∥] Bo Xu,[‡,∥] Dongqin Bi,[†] Haining Tian,*[,‡] Gerrit Boschloo,[†] Licheng Sun,[‡,§] Anders Hagfeldt,[†,§] and Erik M. J. Johansson*[,†]

[†]Department of Chemistry-Ångström Laboratory, Uppsala University, Sweden

[‡]Department of Organic Chemistry, School of Chemical Science and Engineering, Royal Institute of Technology, Stockholm, Sweden

[§]State Key Laboratory of Fine Chemicals, DUT-KTH Joint Research Centre on Molecular Devices, Dalian University of Technology (DUT), 116024 Dalian, China

Supporting Information

ABSTRACT: Efficient solid state dye-sensitized solar cells (sDSCs) were obtained using a small hole transport material, MeO-TPD (*N*,*N*,*N*′,*N*′-tetrakis(4-methoxyphenyl)benzidine), after an initial light soaking treatment. It was discovered that the light soaking treatment for the MeO-TPD based solar cells is essential in order to achieve the high efficiency (4.9%), which outperforms spiro-OMeTAD based sDSCs using the same dye and device preparation parameters. A mechanism based on Li^+ ion migration is suggested to explain the light soaking effect. It was observed that the electron lifetime for the MeO-TPD based sDSC strongly increases after the light soaking treatment, which explains the higher efficiency. After the initial light soaking treatment the device efficiency remains considerably stable with only 0.2% decrease after around 1 month (unsealed cells stored in dark).

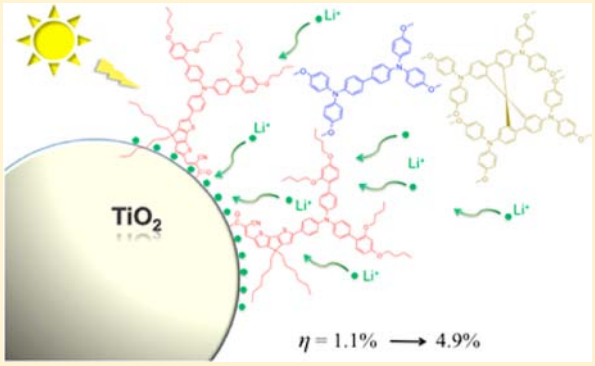

1. INTRODUCTION

The dye-sensitized solar cell (DSC) has emerged as promising alternative photovoltaic devices to the conventional solar cells in terms of cost-efficient fabrication.[1] Also the DSC can be made as a solid state device, "solid-state DSC" (sDSC), probably with practical advantages.[2−4] Upon light excitation, sensitizers separate charge carriers by injecting photoinduced electrons into the conduction band of a mesoporous semiconducting electrode, usually composed of titania nanoparticles, followed by regeneration of the oxidized sensitizers by hole injection into the hole transport material (HTM). The electrons are subsequently conducted through the mesoporous network to the contact and then to the external circuit for electric work. Meanwhile the holes are transferred through the HTM layer to complete the circuit. On the other hand, two recombination processes are suppressing the device performance, namely the charge carrier recombination between the injected electrons with either oxidized sensitizers or the holes in HTM, where the latter usually accounts for the main recombination pathway in sDSCs. To date, the highest certified power conversion efficiency of 6.08% in sDSCs was achieved by using a custom-synthesized dye and the dominating HTM termed 2,2′,7,7′-tetrakis(*N*,*N*-dimethoxyphenylamine)-9,9′-spirobifluorene, spiro-OMeTAD (Figure 1).[5] Recently by doping spiro-OMeTAD with small portion of a cobalt complex, a new record efficiency of 7.2% was obtained.[6] However, in terms of

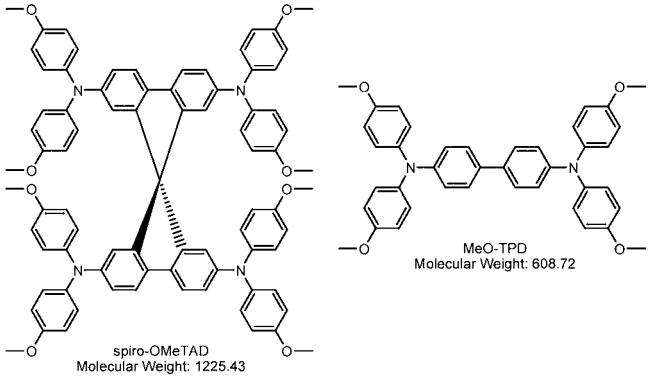

Figure 1. Molecular structures of spiro-OMeTAD and MeO-TPD.

molecular structure and physical properties, the use of spiro-OMeTAD introduces certain limitations to device performance. Such a molecular structure based on the twisted center of the spiro-carbon significantly inhibits the intra- (between the two moieties connected via the spiro center) and intermolecular $\pi-\pi$ conjugation, which results in a fairly low hole-mobility of 4×10^{-5} cm^2 $V^{-1}s^{-1}$ and therefore rather poor performance of hole-conduction.[7] In addition, incomplete pore filling of spiro-

Received: April 4, 2013
Published: April 24, 2013

OMeTAD into the mesoporous electrodes was reported,[8] which may be due to the rather low solubility in organic solvents on account of its large molecular weight. These drawbacks induce high probability of recombination, which lowers the charge collection efficiency. Therefore, alternative HTMs with better hole-conductivity and solubility might be advantageous. Moreover, the high synthetic cost of spiro-OMeTAD is another problem in terms of industrialization of sDSCs. Thus, to design other HTMs overcoming these shortages is very important for the development in this research area in order to obtain low cost devices with better performance. After numerous efforts of pursuing alternative HTMs during 15 years since the discovery of spiro-OMeTAD, ultimately, a small organic HTM was reported, achieving an impressive power conversion efficiency of 2.94%, highlighting the possibility to develop better HTMs for sDSCs.[7]

In this Article, we investigate the sDSCs based on an organic small-molecule HTM termed as *N*,*N*,*N*′,*N*′-tetrakis(4-methoxyphenyl)benzidine, MeO-TPD (also named TMeO-TPD, TPD3 or X1, see Figure 1),[9] with inexpensive synthetic scheme, higher solubility and hole mobility compared to spiro-OMeTAD.

It has been observed that MeO-TPD can be used as HTM in solar cells although the efficiency was not very high.[9] In this report we describe how a light soaking treatment is essential for obtaining a higher efficiency. By treating the devices under simulated AM 1.5G illumination at open-circuit condition for 30 min, the efficiency is increased more than 4 times. After light soaking treatment sDSCs based on MeO-TPD outperform spiro-OMeTAD based devices in spite of the poor initial device performance. We have obtained a record power conversion efficiency (η) of 4.9% in a 2.2 μm thick film of mesoporous TiO_2 device by utilizing an organic dye coded LEG4 (Figure 2)

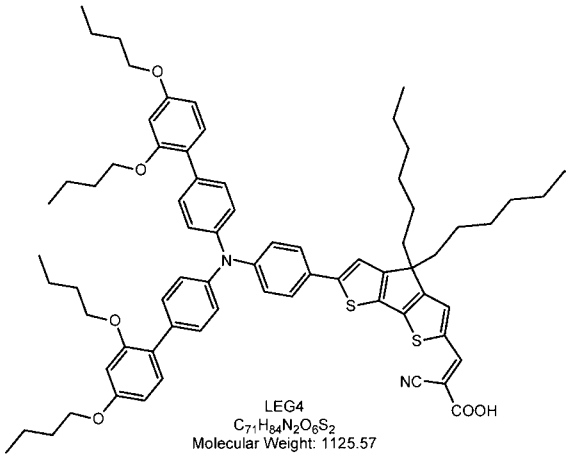

Figure 2. Molecular structure of sensitizer LEG4.

together with MeO-TPD. Thus MeO-TPD is one of the best organic small-molecule HTMs in sDSCs ever reported. Furthermore, there is no presence of other additives or oxidants than the standard *t*-BP and LiTFSI required for these devices to function.

Moreover, after the light soaking treatment, maximal efficiency retains at a nearly similar level for at least 1 month, which shows that the process occurring during the light-soaking treatment improved the device performance to a stable level.

It has previously been observed that light soaking treatment can increase the efficiency of titania based liquid electrolyte DSCs.[10−12] Moreover, recently it was observed that light soaking also affects SnO_2 based sDSCs with spiro-OMeTAD.[13] For SnO_2 based sDSCs, this effect was interpreted in terms of changes on the SnO_2 surface and energy level alignment. For the TiO_2 based liquid electrolyte DSCs, surface ion effects or other mechanisms have also been discussed.[10−12] Moreover, the effect of Li^+ ions on TiO_2 surface or oxidation of spiro-OMeTAD under illumination has been discussed as well.[14,15] Since only TiO_2 was used in this report, we observe different light soaking effects for the sDSCs with different HTMs. The specific nature of the HTM is essential, which requires in-depth characterizations and analysis to be fundamentally understood. The discovery is very important for future development of sDSC with different HTMs. Therefore, we further discuss this phenomenon in terms of Li^+ migration toward the TiO_2 surface in presence of the different HTMs. It might be the case that many of the inapplicable HTMs previously tested in sDSC could probably exhibit better performance if treated by light soaking in combination with Li^+ salts.

As has been investigated for hole transport layer in OLED (organic light emitting diode), MeO-TPD is already commercially available with rather low cost.[16] So far the solubility of HTMs in organic solvents still remains a significant issue since spin-coating is considered as the most feasible method for introducing the HTM into sDSC devices. Moreover, in terms of alternative preparation methods, such as screen-printing and spray deposition that may be promising in future solar cell production, solubility will become an extremely important issue as well. With the molecular weight less than one-half of that for spiro-OMeTAD, MeO-TPD indeed shows an excellent solubility of more than 600 mM in chlorobenzene, the commonly used organic solvent for spin-coating, while the spiro-OMeTAD solution is limited by around 300 mM. The higher solubility may result in better pore filling according to the proposed infiltration mechanism inside mesoporous electrodes.[8,17,18] For an advantageous HTM, high hole-mobility is also required for efficient hole-conduction throughout the electrode in order to successfully extract the charge carriers. As previously reported, the hole-mobility μ of 1×10^{-3} cm^2 V^{-1} s^{-1} for MeO-TPD[7,19−22] is around 2 orders of magnitude higher than that of spiro-OMeTAD. Consequently, MeO-TPD may provide better photovoltaic performance than the previous dominating HTM spiro-OMeTAD in terms of higher power conversion efficiency, higher IPCE, faster charge transport, and better charge collection efficiency, as shown below.

2. EXPERIMENTAL SECTION

Device Fabrication. Samples were prepared on FTO-coated glass substrate purchased from Pilkington (15 Ω/□; 2.3 mm thick; high transparency). First of all, a compact TiO_2 blocking layer was deposited onto the precleaned FTO substrate on hot plate at 450 °C by spray pyrolysis using an air brush at a distance of 5 cm, and the thickness was controlled by 10 spray cycles as standard parameter. The solution used in the spray pyrolysis contains 0.2 M Ti-isopropoxide and 2 M acetylacetone in isopropanol. Nanoporous TiO_2 films were prepared above the blocking layer by spin-coating of a colloidal TiO_2 paste (Dyesol DSL 18NR-T) containing nanoparticles in the order of 20 nm in average diameter diluted with terpineol (46.2% in weight ratio). The spin-coating rate of 2400 rpm for 30 s was adopted to obtain about 2.2 μm thick nanoporous film, as measured with DekTak profilometer and SEM. After sintering the TiO_2 film on hot plate at 500 °C for 30 min, the film was cooled to room temperature and immersed in 0.02 M aqueous $TiCl_4$ at 70 °C for 30 min. The film was

dx.doi.org/10.1021/ja403344s | J. Am. Chem. Soc. 2013, 135, 7378−7385

then rinsed with deionized water and again annealed on hot plate at 500 °C for 30 min followed by dye-sensitization in a solution of 0.5 mM LEG4 in MeCN for 18 h. For samples with spiro-OMeTAD as HTM, a solution of 150 mM spiro-OMeTAD (Lumtech) (213 mg/mL), 120 mM 4-*tert*-butylpyridine and 20 mM $LiN(CF_3SO_2)_2$ in chlorobenzene was applied to the films by leaving the solution to penetrate into the films for 30 s and then spin-coating for 30 s with 2000 rpm. For samples based on MeO-TPD (custom-synthesized[10]), a solution of 158 mM MeO-TPD, 158 mM 4-*tert*-butylpyridine, and 128 mM $LiN(CF_3SO_2)_2$ in chlorobenzene was prepared in an argon glovebox prior to spin-coating. For comparison, another solution of 158 mM spiro-OMeTAD was prepared with 4-*tert*-butylpyridine and $LiN(CF_3SO_2)_2$ both in the same molar ratio as applied for MeO-TPD solution. The solution afterward was applied to the films by spin-coating in the same way. Finally, a 200 nm thick Ag (Sigma-aldrich; ≥ 99.99% trace metals basis) contact was deposited onto the organic semiconductor by thermal evaporation in a vacuum chamber (Leica EM MED020) with a base pressure of about 10^{-5} mbar, to complete the device. All measurements were performed on devices within 1 week after device preparation, except for the long-term stability measurements.

UV−vis Spectroscopy. UV−Visible absorption spectra of sensitized TiO_2 films were recorded on an HR-2000 Ocean Optics fiber optics spectrophotometer.

Incident Photon to Current Conversion Efficiency (IPCE). IPCE spectra were recorded on a computer-controlled setup comprising a xenon lamp (Spectral Products ASB-XE-175), a monochromator (Spectral Products CM110), and a potentiostat (EG&G PAR 273). The equipment was calibrated with a certified silicon solar cell (Fraunhofer ISE) prior to measurements. All sDSC samples were illuminated from a glass side with an aperture area of 0.16 cm^2 (0.4 × 0.4 cm^2).

Photocurrent Density−Voltage Measurement. The light source of solar simulator for measuring current−voltage characteristics was a 300 W collimated xenon lamp (Newport) calibrated with the light intensity to 1000 W m^{-2} at 1.5 a.m. Global condition by a certified silicon solar cell (Fraunhofer ISE). Electrical data was recorded on a computer controlled by a digital sourcemeter (Keithley model 2400) with the scan direction from open-circuit short-circuit at 11.9 mV/s. The prepared sDSC samples were masked during the measurement with an aperture area of 0.20 cm^2 (0.4 × 0.5 cm^2) exposed under illumination.

Photocurrent and Voltage Decay Measurements. Transient photovoltage and photocurrent decay as a function of light intensity were measured by the custom-made "toolbox setup" using a white LED (Luxeon Star 1W) as light source to provide the base light intensity. The transient voltage and current response of the cells were recorded by using a 16-bit resolution digital acquisition board (National Instruments) in combination with a current amplifier (Stanford Research Systems RS570) and a homemade electromagnetic switching system.

By superimposing the base light with a small square wave modulation (<10%, 0.5 Hz), the transient photovoltage was recorded and subsequently fitted into a first-order kinetics to extract the time constants corresponding to the electron lifetimes.

3. RESULTS AND DISCUSSION

Based on the features and structure of sensitizer D35,[23,24] the extra thiophene group built into a more rigid and planar molecular structure as linker broadens the absorption spectrum of LEG4 (purchased from Dyenamo) with a red-shift. As can be seen in Figure 3, the photocurrent contributing to the IPCE spectra is mainly attributed to the absorption of sensitizer roughly from 400 to 650 nm with no contribution from hole-conductors since neither MeO-TPD (see Figure S1 in the Supporting Information) nor spiro-OMeTAD absorbs in this region.

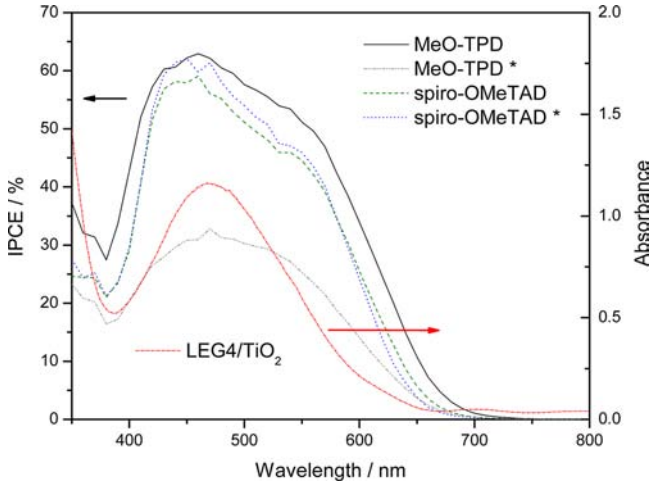

Figure 3. Absorption spectrum of sensitizer LEG4 on around 1 μm thin mesoporous TiO_2 electrode (red dash dotted trace) and IPCE spectra for sDSCs based on two organic HTMs: the cell using 158 mM MeO-TPD, 158 mM *t*-BP, and 128 mM LiTFSI after light soaking treatment (black solid trace) and before light soaking treatment (gray dash dot dotted trace), the cell using 158 mM spiro-OMeTAD, 158 mM *t*-BP, and 128 mM LiTFSI (green dashed trace), the cell using 150 mM spiro-OMeTAD, 120 mM *t*-BP, and 20 mM LiTFSI (blue dotted trace).

The sDSC using MeO-TPD after the light soaking treatment exhibits the highest IPCE of 63% at the maximum absorption wavelength of 460 nm, which is in agreement with the maximal absorption wavelength of the dye molecule on the TiO_2 surface. The devices based on spiro-OMeTAD with additives using either standard or same concentration adopted for MeO-TPD based devices display both slightly lower IPCE spectra but with the similar spectral shapes and curvature. This indicates that there is a larger loss over the total spectral region in the sDSCs with spiro-OMeTAD in comparison to the sDSCs based on MeO-TPD. Before the light soaking treatment the MeO-TPD based sDSC shows much lower IPCE than after the light soaking treatment. This effect is therefore studied in more detail below.

In agreement with IPCE spectra, the MeO-TPD based device with optimized additive (*t*-BP and LiTFSI) concentrations provides the highest J_{sc} of 9.5 mA cm^{-2} (Table 1 and Figure 4) after the light soaking treatment, which exceeds those for spiro-OMeTAD based cells with additive concentrations as either reported previously[5] or with the same values as tested with MeO-TPD. The integrated short circuit photocurrent density for the sDSC based on MeO-TPD was calculated from the

Table 1. Data of *I*−*V* Characteristics for sDSCs Based on Two Organic HTMs[a]

sDSC	V_{oc}/mV	J_{sc}/mA cm^{-2}	FF/%	η/%
MeO-TPD	800	9.5	65	4.9
MeO-TPD*	750	2.7	55	1.1
spiro-OMeTAD	860	8.9	62	4.7
spiro-OMeTAD*	880	9.2	56	4.6

[a]MeO-TPD* denotes characteristics for the device before the light soaking treatment. Spiro-OMeTAD denotes the characteristics for the cell using 158 mM spiro-OMeTAD, 158 mM *t*-BP, and 128 mM LiTFSI. Spiro-OMeTAD* denotes the characteristics for the cell using 150 mM spiro-OMeTAD, 120 mM *t*-BP, and 20 mM LiTFSI.

dx.doi.org/10.1021/ja403344s | J. Am. Chem. Soc. 2013, 135, 7378−7385

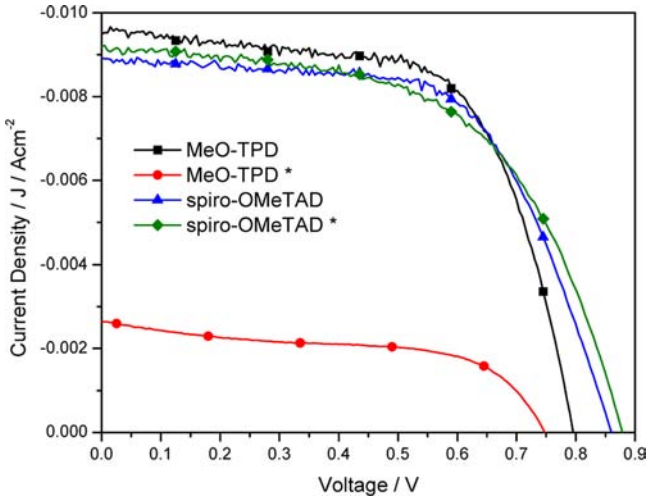

Figure 4. *I*–*V* characteristics for sDSCs based on two organic HTMs: the cell using 158 mM MeO-TPD, 158 mM *t*-BP, and 128 mM LiTFSI after light soaking treatment (black trace with square), the cell using 158 mM MeO-TPD, 158 mM *t*-BP, and 128 mM LiTFSI before light soaking treatment (red trace with circle), the cell using 158 mM spiro-OMeTAD, 158 mM *t*-BP, and 128 mM LiTFSI (blue trace with uptriangle), the cell using 150 mM spiro-OMeTAD, 120 mM *t*-BP, and 20 mM LiTFSI (green trace with diamond).

IPCE spectra in Figure 3 to about 8 mA cm^{-2}, which is slightly lower than the J_{sc} measured from *I*–*V* curves, which may be a result of the significantly lower intensity of the light source for IPCE measurements and a slightly nonlinear device characteristics (see Figure S3 in the Supporting Information). In addition, some of the devices based on MeO-TPD even display J_{sc} over 10 mA cm^{-2} but with slightly lower power conversion efficiency.

Compared to spiro-OMeTAD, MeO-TPD has a rather similar HOMO level of 5.1 eV.[25,26] However, the spiro-OMeTAD based devices exhibit higher open circuit voltage V_{oc} by up to 80 mV over the V_{oc} of 800 mV for MeO-TPD based device probably due to the slightly longer electron lifetime at open circuit as discussed further below. Moreover, compared to the spiro-OMeTAD based device with higher LiTFSI concentration, slightly higher V_{oc} was also observed for the device using standard concentration of LiTFSI and spiro-OMeTAD. This may be an effect of the shifted TiO_2 energy levels due to more Li^+ ions adsorbed at the TiO_2 surface, which generally results in V_{oc} changes for DSCs.[27] On the other hand the MeO-TPD based device shows a better fill factor than those of the devices using spiro-OMeTAD, which is probably due to that MeO-TPD based device structure appears with the lowest series resistance observed in the slopes of the IV curves in the vicinity of open circuit condition. It is commonly considered that charge carrier transport commences to become the most dominant limitation when the device operates at close to open circuit condition due to significant probability of charge recombination. Therefore it might be inferred that faster charge transport and higher charge collection efficiency are specifically important for devices based on MeO-TPD.

The comparison in *I*–*V* characteristics of MeO-TPD based devices before and after light soaking treatment unambiguously illustrates that all photovoltaic parameters have been considerably improved, particularly J_{sc} enhanced most dramatically from 2.7 to 9.5 mA cm^{-2}. In contrast, such a behavior was not observed for spiro-OMeTAD based devices in spite of certain negligible fluctuation in photovoltaic parameters.

The highly interesting discovery that the efficiency of MeO-TPD based device increases upon light soaking is monitored in more detail in Figure 5. The devices were treated with simulated AM 1.5G 100 mW cm^{-2} illumination at open circuit and the device efficiency were measured at different durations of this treatment.

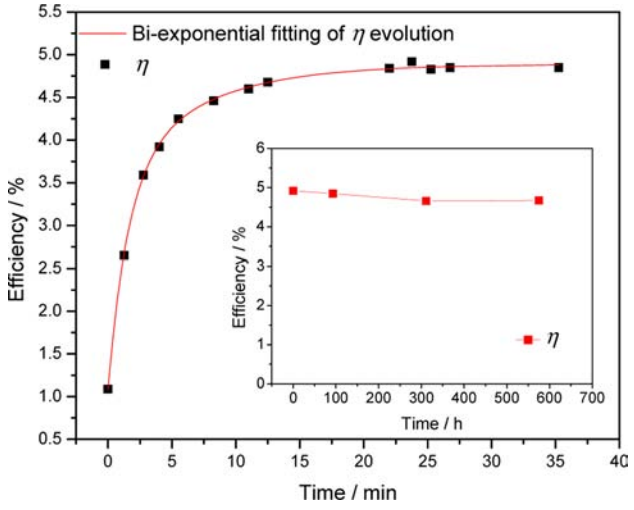

Figure 5. Power conversion efficiency η of MeO-TPD based device fitted with a biexponential function of time under light soaking treatment at open circuit (AM 1.5G, 100 mW cm^{-2}). The inset displays the evolution of η over barely 1 month after light soaking treatment when unsealed devices were stored at room temperature in dark and in air with low humidity (below 15%).

As clearly shown in Figure 5, it can be concluded that the power conversion efficiency increases dramatically as a function of time under the light soaking treatment. Initially, the device only provides conversion efficiency of 1.1% followed by a rapid increase all the way to 4.9% in a biexponential functional curvature (see the Supporting Information for detailed information about solar cell performance development). Moreover, the power conversion efficiency remains impressively stable after the initial light soaking treatment with only 0.2% drop over 580 h, nearly 1 month, in unsealed devices stored at room temperature in dark air with low humidity (Figure 5, inset).

To understand this phenomenon, we investigate the effect of different conditions on these devices. Storage in darkness and light soaking treatment at short circuit condition both resulted in negligible enhancement of photovoltaic performance, which implies that light soaking at open circuit condition is the most efficient treatment for improving the performance of MeO-TPD based devices; that is, light alone does not result in the increased performance, since the enhancement was negligible under illumination at short-circuit compared to open-circuit. Therefore, the local potential obtained during the light soaking at open-circuit seems to be essential. To investigate this effect a potential similar to V_{oc} was applied upon the sDSC in dark, which also induces an increase of the device performance. While for a reverse potential applied in dark no increase in the performance was observed.

In order to understand more about the effect behind the enhancement of the photovoltaic performance after the light

dx.doi.org/10.1021/ja403344s | *J. Am. Chem. Soc.* 2013, 135, 7378–7385

soaking treatment, transient photovoltage decay measurements and transient photocurrent decay measurements were performed in comparison to spiro-OMeTAD devices.

Transient photovoltage decay measurements indicate how fast injected electrons can recombine, from which the electron lifetime (τ_e) can be extracted. As shown in Figure 6, the

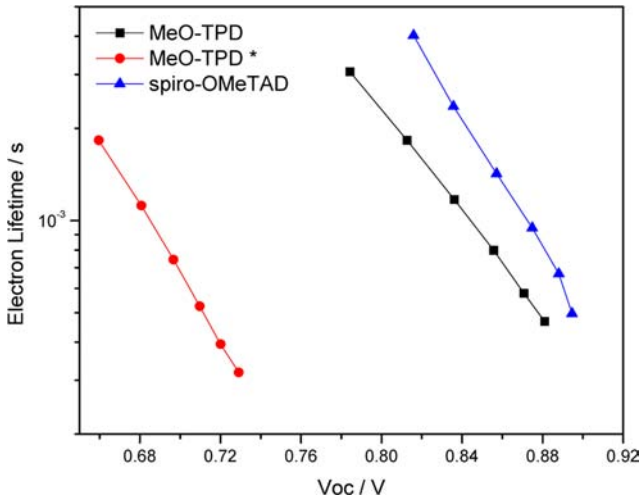

Figure 6. Electron lifetime in correlation with V_{oc} for sDSCs based on two organic HTMs: the cell using 158 mM MeO-TPD, 158 mM *t*-BP, and 128 mM LiTFSI after light soaking treatment (black trace with square), the cell using 158 mM MeO-TPD, 158 mM *t*-BP, and 128 mM LiTFSI before light soaking treatment (red trace with circle), and the cell using 158 mM spiro-OMeTAD, 158 mM *t*-BP, and 128 mM LiTFSI (blue trace with triangle).

electron lifetime for the device based on spiro-OMeTAD is slightly longer compared to the device based on MeO-TPD (after light soaking treatment). The longer electron lifetime implies a higher electron concentration at light illumination, and the device therefore shows a slightly higher electron quasi-Fermi level in titania compared to the MeO-TPD based device. This may be the reason why MeO-TPD based devices after the light soaking treatment also display a slightly lower V_{oc} compared to the spiro-OMeTAD based devices in the *I*–*V* characteristics (Figure 4). Generally, in the sDSC devices sensitized by a triphenylamine based D-π-A dye, the recombination of injected electrons with holes in the HTM layer usually accounts for the dominating recombination pathway. The titania surface is partly protected by the hydrophobic alkyl chains introduced at the donor terminal of the dye molecule stretching outward into the pores where HTM is located. However, with the smaller and more flexible structure compared to spiro-OMeTAD, MeO-TPD might be located much closer to the titania surface (see Abstract figure). This definitely results in slightly higher recombination probability and therefore lower electron lifetime, which then lowers the V_{oc} as shown in the *I*–*V* curves.[28]

On the other hand, the MeO-TPD based device displays a significant enhancement in the electron lifetime after the light soaking treatment. The extremely short electron lifetime before the light soaking treatment induces markedly low V_{oc} and poor conversion efficiency since the majority of injected electrons rapidly recombine with holes located on the oxidized HTM. Two different processes may be discussed in relation to this phenomenon: the HTM is oxidized, or/and Li^+ ions migrate inside the pores. Provided MeO-TPD molecules are partially oxidized under illumination, even faster recombination would be expected since higher concentration of oxidized HTM boosts recombination ultimately yielding even shorter charge carrier lifetime, which apparently contradicts the experimental observation. Thus, we hereby propose the viable hypothetical mechanism that Li^+ ions tend to migrate from certain coordinates inside the pores toward the titania/sensitizer interface driven by the local electric field induced after photoexcitation and charge separation at open circuit (see Abstract figure). It is well established that Li^+ ions as additive for HTM are necessary for sDSC devices to function.[29] This is partially attributed to that positively charged Li^+ ions tend to adsorb onto the negatively charged titania surface to compensate and screen conduction band electrons after injection, and therefore inhibit charge recombination.[30]

To certify the hypothesis proposed above, the complete devices have been made and tested under light soaking treatment without LiTFSI but using the same concentrations of HTMs and *t*-BP as adopted for those devices with record efficiencies. As shown in the inset of Figure 7, the device based

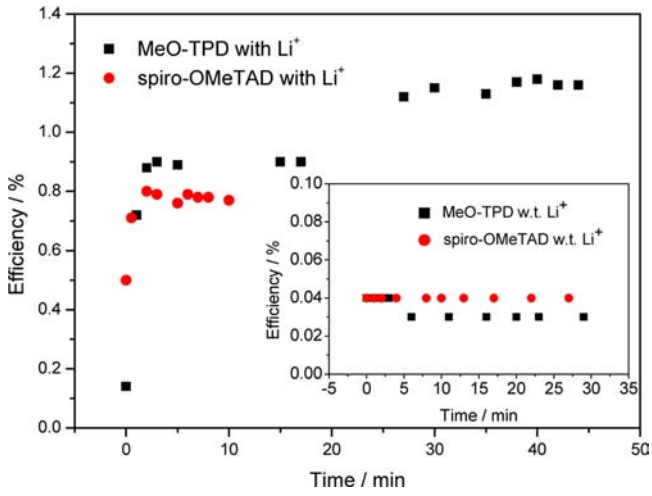

Figure 7. Evolution of power conversion efficiencies as a function of time under light soaking treatment: the cell using 158 mM MeO-TPD and 158 mM *t*-BP (black trace with square), the cell using 158 mM spiro-OMeTAD and 158 mM *t*-BP (red trace with circle); on both solar cells, a solution of 1 M LiTFSI was afterward spin-coated on top of the complete devices. Inset: the cell using 158 mM MeO-TPD and 158 mM *t*-BP without LiTFSI (black trace with square), the cell using 158 mM spiro-OMeTAD and 158 mM *t*-BP without LiTFSI (red trace with circle).

on either MeO-TPD or spiro-OMeTAD provides almost no efficiency with a constant value around 0.03% or 0.04%, which clearly shows that the device can hardly function[29] and the photovoltaic performance is independent of light soaking treatment in the absence of LiTFSI. However, both devices exhibit the same interesting phenomenon as observed previously when a solution of 1 M LiTFSI in MeCN was spin-coated on top of these devices (on top of the completed devices).

As can be seen in Figure 7, the efficiencies of both devices have been improved dramatically under light soaking condition in the presence of LiTFSI introduced into the top of the devices. Thus, it is clearly observed that the same device behaves in completely different ways under light soaking with or without LiTFSI. Therefore we can infer that such a light-

dx.doi.org/10.1021/ja403344s | *J. Am. Chem. Soc.* 2013, 135, 7378–7385

soaking phenomenon is due to the Li+ migration effect inside the porous electrode since there is no difference between the devices in parallel comparison respectively except for the presence of LiTFSI.

During the standard device fabrication, the HTM and additives are well mixed prior to infiltrating into the mesoporous electrode within the solution and eventually remain randomly distributed inside the pores when penetration ceases as soon as the solvent evaporates.[8,17,18] A local electric field across the device is established when the two quasi-Fermi levels are shifted toward separate directions by electron and hole injections upon illumination,[31,32] which is therefore instantaneously followed by the migration of Li^+ ions toward titania surface due to the Coulombic interaction. The higher potential, the stronger driving force, and therefore the faster migration proceeds.

As discussed above for the suggested model, the built-in potential under open-circuit conditions, namely, the V_{oc}, should be the essential driving force rather than light soaking treatment if the improvement in device performance is really due to the Li^+ ion migration toward titania/sensitizer interface resulting in stronger suppression of recombination. To investigate such an argument, a negative bias potential by 20 mV higher than the absolute value of V_{oc} of each individual device was applied in darkness across the cell using 158 mM HTM (either MeO-TPD or spiro-OMeTAD) and 158 mM *t*-BP with 1 M LiTFSI spin-coated on top of the device. The evolution of power conversion efficiency of each device as a function of time was monitored and recorded in Figure 8, which apparently displays the similar observations for devices based on both HTMs.

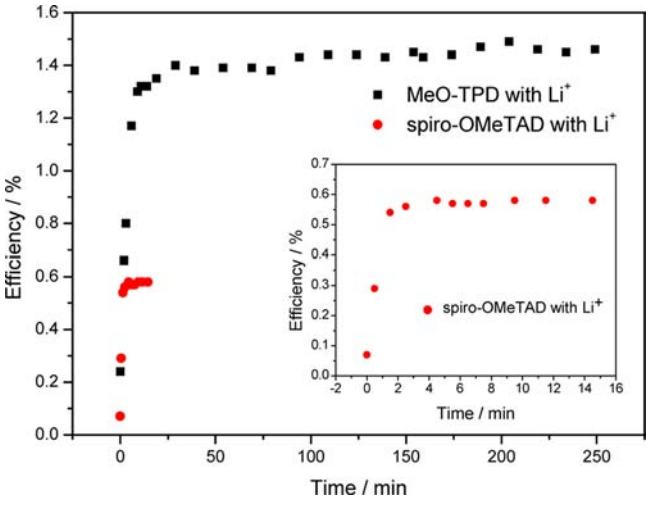

Figure 8. Evolution of power conversion efficiencies as a function of time under applied potential treatment: the cell using 158 mM MeO-TPD and 158 mM *t*-BP (black trace with square), the cell using 158 mM spiro-OMeTAD and 158 mM *t*-BP (red trace with circle); on both solar cells, a solution of 1 M LiTFSI was afterward spin-coated on top of the complete devices. Inset: the magnification for the spiro-OMeTAD based cell (red trace with circle).

The photovoltaic performance is significantly improved when the device is subject to applied potential in darkness, which distinctly indicates that the light-soaking effect is attributed to the Li^+ ion migration by the electric field built in the solar cell during illumination as driving force.

Moreover, the same trend has been observed again as discussed in all previous experiments that the device performance of MeO-TPD based cells undergoes much longer time to reach its maximum state compared with spiro-OMeTAD based cells. We suggest that such a time difference is due to the difference in ion migration process through the hole transport material. The ion migration might suffer from steric hindrance by the variation of molecular structures of the hole transport material, such as spiro-OMeTAD and MeO-TPD. With relatively weak $\pi-\pi$ stacking in virtue of the twisted conformation, the former HTM provides higher freedom for diffusion in three dimensions with both intra- and intermolecular pathways, which leads to swift ion migration within a negligible time domain, and therefore, the light soaking effect can barely be observed. While with predictably strong intermolecular $\pi-\pi$ stacking on account of highly rigid and planar structure, MeO-TPD can block feasible pathways for ion diffusion, which may slower migration of Li^+ ions. It is also notable that the devices shown in Figures 7 and 8 using no matter MeO-TPD or spiro-OMeTAD always exhibit much longer time for efficiency evolution to its maximal level than those with record efficiencies such as the one shown in Figure 5. This is probably due to that LiTFSI was applied by spin-coating after the fabrication of the complete device. In this case, Li^+ ions were only introduced into the top of the complete device, since the solution was spin-casted away with only a few seconds waiting time after addition. When the device is subject to either illumination at open circuit or applied potential in darkness, the Li^+ ions need much more time to first penetrate the overstanding HTM layer and then porous electrode filled by HTM and *t*-BP on their way toward the negatively charged titania/sensitizer interface. However, in the previous case, when the LiTFSI was mixed into the HTM solution, the Li^+ ions were already infiltrated into the pores collectively with HTM and *t*-BP before light soaking treatment, which therefore underwent shorter time for efficiency evolution. For spiro-OMeTAD based devices, this occurred within an almost negligible time domain, which explains why it was considerably difficult to observe the light-soaking effect for the spiro-OMeTAD based devices when the LiTFSI was mixed into the spiro-OMeTAD solution prior to infiltration.

The light-soaking effect was observed in MeO-TPD based devices for different Li^+ ion concentrations. As shown in Figure 9, efficiency increase is a general observation for these devices when the concentration of LiTFSI is altered in a large range. Furthermore, it can be seen obviously that the device with higher Li^+ ion concentration provides better power conversion efficiency at its maximal state than those with lower Li^+ ion concentrations although it reaches its optimal photovoltaic performance within a longer time domain.

With more Li^+ ions inside the device, more time is needed for the majority of Li^+ migrating to reach the titania/sensitizer interface, but with higher concentration of Li^+ ions it is also observed that the efficiency is increased more during the light soaking treatment. The increased electron lifetime after light soaking due to Li^+ ion migration to the TiO_2 surface as discussed previously explains why the efficiency is further increased with higher Li concentration. According to the proposed mechanism, the efficiency evolution under light soaking should be readily ceased by imposing a positive bias potential at the same time across the device, which is also eventually proven to be true as expected. The evolving process of power conversion efficiency of the device can be terminated and the efficiency can be maintained at the transient level when a positive bias potential equal to V_{oc} was employed. All these

dx.doi.org/10.1021/ja403344s | J. Am. Chem. Soc. 2013, 135, 7378−7385

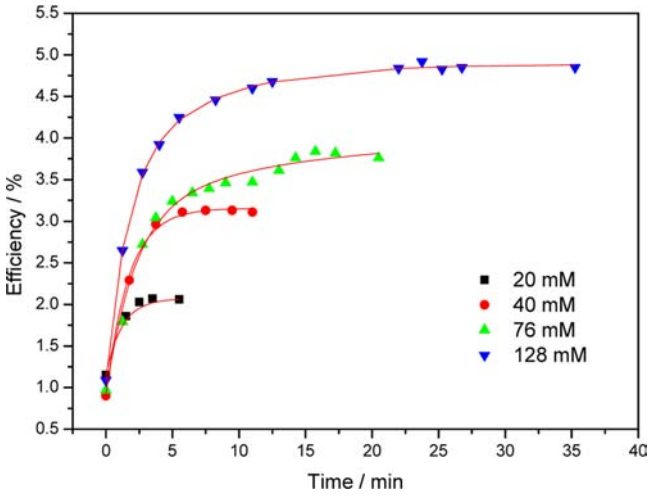

Figure 9. Evolution of power conversion efficiencies as a function of time under light soaking treatment for the devices using 158 mM MeO-TPD, 158 mM *t*-BP, and a series of different concentrations of LiTFSI: 20 mM (black trace with square), 40 mM (red trace with circle), 76 mM (green trace with up-triangle), and 128 mM (blue trace with down-triangle).

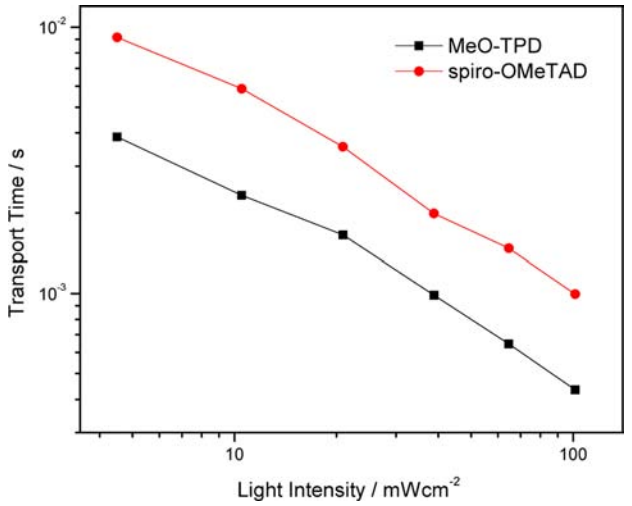

Figure 10. Transport time in correlation with light intensity for sDSCs based on two organic HTMs: the cell using 158 mM MeO-TPD, 158 mM *t*-BP, and 128 mM LiTFSI after light soaking treatment (black trace with square), the cell using 158 mM spiro-OMeTAD, 158 mM *t*-BP, and 128 mM LiTFSI (red trace with circle).

results discussed above highly agree with the proposed model and delicately interpret the mechanism behind the light-soaking effect.

As already discussed for the experiments with a variety of different treatments, light soaking at open circuit was found the most efficient method to improve device performance and an increase was also found when applying a voltage (similar to V_{oc}) in dark. These results are therefore in agreement with the model proposed above based on Li^+ ion migration toward the negatively charged TiO_2 surface.

What's more, as clearly shown in Figure 5, the evolution of η under light soaking follows a biexponential function of time comprising two components, where the first (faster) may be limited by diffusion of Li^+ ions while the second (slower) may be limited by the decreased concentration of Li^+ ions away from the titania surface. Hence, we suggest that the improvement of power conversion efficiency and photovoltaic parameters in MeO-TPD based devices by the open-circuit light soaking treatment is observed due to the strong enhancement of electron lifetime by Li^+ ions migration occurring at the nanostructural interfaces of mesoporous titania electrodes.

The light-soaking effect with LiTFSI seems to be rather general for sDSC devices based on different HTMs. In addition to MeO-TPD and spiro-OMeTAD, we have also found an impressive improvement in efficiency for devices with another HTM, tris(para-anisyl)amine. Previously, this HTM only showed considerably low efficiency of 0.07% in the devices;[33] however, by using light soaking treatment, we have now observed the same effect in this system that the efficiency has been increased up to above 1.5% after the treatment. We therefore think that such a light-soaking treatment with LiTFSI may be a general way to improve the sDSC, and will therefore be very important to be considered in the future development of new HTMs and the optimizations for solid-state DSCs.

The transport time dependent on light intensity is displayed in Figure 10 (see the Supporting Information for details). It may clearly be observed in the graph that the electron transport time of MeO-TPD based devices is less than 1/3 of that for the devices using spiro-OMeTAD. As suggested from the mobility data of MeO-TPD and spiro-OMeTAD, and the $I-V$ measurements discussed above, it is not surprising that the charge transport is faster in the sDSC with MeO-TPD.

According to the Einstein equation, D_{eff} is subject to the expression:

$$D_{eff} = k_B T \mu_{eff} / q$$

where D_{eff} represents effective diffusion coefficient, k_B stands for Boltzmann constant, T designates temperature, μ_{eff} denotes effective mobility comprising contributions from both charge carriers (electrons and holes), and q is the elementary charge. Moreover, D_{eff} can also be estimated from τ_{trans} and device thickness w by the following equation:[34]

$$D_{eff} = w^2/(2.35\tau_{trans})$$

Rearrangement gives the correlation between μ_{eff} and τ_{trans} by the following expression:

$$\mu_{eff} = D_{eff} q/(k_B T) = w^2 q/(2.35 k_B T \tau_{trans})$$

Here we can assume that the electron-mobility is similar for both spiro-OMeTAD and MeO-TPD based devices, since they are fabricated according to completely the same protocol only except for the HTMs. Therefore, the contribution of hole-mobility to μ_{eff} can be correlated to τ_{trans} by the equation, which indicates that higher hole-mobility of HTM truly results in faster charge transport throughout the solar cell as observed for MeO-TPD based devices. Moreover, faster charge transport in association with competitive electron lifetime eventually contributes to the higher charge collection efficiency for the devices based on MeO-TPD compared to spiro-OMeTAD (see the Supporting Information for charge collection efficiency).

4. CONCLUSIONS

In summary, with higher solubility and higher hole-mobility a small-molecule organic hole transport material MeO-TPD outperforms the dominating HTM spiro-OMeTAD in sDSC devices by providing better power conversion efficiency and photovoltaic parameters in terms of competitive electron lifetime, faster charge transport and higher charge collection

dx.doi.org/10.1021/ja403344s | J. Am. Chem. Soc. 2013, 135, 7378−7385

efficiency. It was discovered that an initial light soaking treatment at open circuit condition significantly improved the device performance to the optimal state and the device efficiency remained considerably stable with only 0.2% decrease in about one month. Electron lifetime and charge transport-time measurements were performed to understand the effect of this light soaking treatment in more detail, and it was observed that the electron lifetime was significantly improved, which explains, at least partly, the increased efficiency. According to these results, a mechanism of device performance evolution depending on Li^+ ion migration toward the surface of TiO_2 nanoparticles under light soaking was suggested. These results provide a promising pathway for developing new small-molecule HTMs alternative to spiro-OMeTAD in sDSCs.

■ ASSOCIATED CONTENT

Supporting Information

Absorption spectrum of MeO-TPD, photocurrent decay measurements, charge collection efficiency, evolution of current−voltage characteristics of MeO-TPD based sDSC after light soaking treatment of different duration. This material is available free of charge via the Internet at http://pubs.acs.org.

■ AUTHOR INFORMATION

Corresponding Author

haininGt@kth.se; erik.johansson@kemi.uu.se

Author Contributions

[‖]L.Y. and B.X. contributed to this work equally.

Notes

The authors declare no competing financial interest.

■ ACKNOWLEDGMENTS

The authors acknowledge the financial support by the Swedish Energy Agency, the Swedish Research Council (VR), the STandUP for Energy program and the Göran Gustafsson Foundation. We thank Kari Sveinbjörnsson for the reference experiment with the HTM tris(para-anisyl)amine and Erik Gabrielsson for dye synthesis.

■ REFERENCES

(1) O'Regan, B.; Grätzel, M. *Nature* **1991**, *353*, 737−740.
(2) Bach, U.; Lupo, D.; Comte, P.; Moser, J. E.; Weissörtel, F.; Salbeck, J.; Spreitzer, H.; Grätzel, M. *Nature* **1998**, *395*, 583−585.
(3) Hagfeldt, A.; Boschloo, G.; Sun, L.; Kloo, L.; Pettersson, H. *Chem. Rev.* **2010**, *110*, 6595−6663.
(4) Snaith, H. J.; Schmidt-Mende, L. *Adv. Mater.* **2007**, *19*, 3187−3200.
(5) Cai, N.; Moon, S.-J.; Cevey-Ha, L.; Moehl, T.; Humphry-Baker, R.; Wang, P.; Zakeeruddin, S. M.; Grätzel, M. *Nano Lett.* **2011**, *11*, 1452−1456.
(6) Burschka, J.; Dualeh, A.; Kessler, F.; Baranoff, E.; Cevey-Ha, N.-L.; Yi, C.; Nazeeruddin, M. K.; Grätzel, M. *J. Am. Chem. Soc.* **2011**, *133*, 18042−18045.
(7) Leijtens, T.; Ding, I.-K.; Giovenzana, T.; Bloking, J. T.; McGehee, M. D.; Sellinger, A. *ACS Nano* **2012**, *6*, 1455−1462.
(8) Melas-Kyriazi, J.; Ding, I.-K.; Marchioro, A.; Punzi, A.; Hardin, B. E.; Burkhard, G. F.; Tétreault, N.; Grätzel, M.; Moser, J.-E.; McGehee, M. D. *Adv. Energy Mater.* **2011**, *1*, 407−414.
(9) Jager, C.; Haarer, D.; Peng, B.; Thelakkat, M. *Appl. Phys. Lett.* **2004**, *85*, 6185−6187.
(10) Gregg, B. A.; Chen, S.-G.; Ferrere, S. *J. Phys. Chem. B* **2003**, *107*, 3019−3029.
(11) Listorti, A.; Creager, C.; Sommeling, P.; Kroon, J.; Palomares, E.; Fornelli, A.; Breen, B.; Barnes, P. R. F.; Durrant, J. R.; Law, C.; O'Regan, B. *Energy Environ. Sci.* **2011**, *4*, 3494−3501.
(12) Wang, Q.; Zhang, Z.; Zakeeruddin, S. M.; Gratzel, M. *J. Phys. Chem. C* **2008**, *112*, 7084−7092.
(13) Tiwana, P.; Docampo, P.; Johnston, M. B.; Herz, L. M.; Snaith, H. J. *Energy Environ. Sci.* **2012**, *5*, 9566−9573.
(14) Cappel, U. B.; Daeneke, T.; Bach, U. *Nano Lett.* **2012**, *12*, 4925−4931.
(15) Scholin, R.; Karlsson, M. H.; Eriksson, S. K.; Siegbahn, H.; Johansson, E. M. J.; Rensmo, H. *J. Phys. Chem. C* **2012**, *116*, 26300−26305.
(16) Walzer, K.; Maennig, B.; Pfeiffer, M.; Leo, K. *Chem. Rev.* **2007**, *107*, 1233−1271.
(17) Ding, I.-K.; Melas-Kyriazi, J.; Cevey-Ha, N.-L.; Chittibabu, K. G.; Zakeeruddin, S. M.; Grätzel, M.; McGehee, M. D. *Org. Electron.* **2010**, *11*, 1217−1222.
(18) Snaith, H. J.; Humphry-Baker, R.; Chen, P.; Cesar, I.; Zakeeruddin, S. M.; Grätzel, M. *Nanotechnology* **2008**, *19*, 424003−424015.
(19) Pfeiffer, M.; Leo, K.; Zhou, X.; Huang, J. S.; Hofmann, M.; Werner, A.; Blochwitz-Nimoth, J. *Org. Electron.* **2003**, *4*, 89−103.
(20) Borsenberger, P. M.; Fitzgerald, J. J. *J. Phys. Chem.* **1993**, *97*, 4815−4819.
(21) Wu, I. W.; Wang, P. S.; Tseng, W. H.; Chang, J. H.; Wu, C. I. *Org. Electron.* **2012**, *13*, 13−17.
(22) Gao, H. *J. Mol. Struct: THEOCHEM* **2010**, *962*, 80−84.
(23) Hagberg, D. P.; Jiang, X.; Gabrielsson, E.; Linder, M.; Marinado, T.; Brinck, T.; Hagfeldt, A.; Sun, L. *J. Mater. Chem.* **2009**, *19*, 7232−7238.
(24) Yang, L.; Cappel, U. B.; Unger, E. L.; Karlsson, M.; Karlsson, K. M.; Gabrielsson, E.; Sun, L.; Boschloo, G.; Hagfeldt, A.; Johansson, E. M. *J. Phys. Chem. Chem. Phys.* **2012**, *14*, 779−789.
(25) Tomita, Y. Ph.D. Thesis, Technischen Universität Dresden, Dresden, Germany, 2005.
(26) He, G.; Walzer, K.; Pfeiffer, M.; Leo, K. *Proc. SPIE* **2004**, *5519*, 42−47.
(27) Liu, Y.; Hagfeldt, A.; Xiao, X.-R.; Lindquist, S.-E. *Sol. Energy Mater. Sol. Cells* **1998**, *55*, 267−281.
(28) Johansson, E. M. J.; Karlsson, P. G.; Sandell, A.; Siegbahn, H.; Rensmo, H. *Chem. Mater.* **2007**, *19*, 2071−2078.
(29) Karthikeyan, C. S.; Thelakkat, M. *Inorg. Chim. Acta* **2008**, *361*, 635−655.
(30) Krüger, J.; Plass, R.; Cevey, L.; Piccirelli, M.; Grätzel, M.; Bach, U. *Appl. Phys. Lett.* **2001**, *79*, 2085−2087.
(31) Cappel, U. B.; Feldt, S. M.; Schoneboom, J.; Hagfeldt, A.; Boschloo, G. *J. Am. Chem. Soc.* **2010**, *132*, 9096−9101.
(32) Ardo, S.; Sun, Y.; Staniszewski, A.; Castellano, F. N.; Meyer, G. J. *J. Am. Chem. Soc.* **2010**, *132*, 6696−6709.
(33) Johansson, E. M. J.; Yang, L.; Gabrielsson, E.; Lohse, P. W.; Boschloo, G.; Sun, L.; Hagfeldt, A. *J. Phys. Chem. C* **2012**, *116*, 18070−18078.
(34) van de Lagemaat, J.; Frank, A. J. *J. Phys. Chem. B* **2001**, *105*, 11194−11205.